Cell

Real-Time Kinetics of Gene Activity in Individual Bacteria

Ido Golding,[1,*] Johan Paulsson,[2,3] Scott M. Zawilski,[1] and Edward C. Cox[1,*]
[1] Department of Molecular Biology, Princeton University, Princeton, NJ 08544, USA
[2] Department of Applied Mathematics and Theoretical Physics, University of Cambridge, Cambridge CB3 0WA, United Kingdom
[3] Present address: Department of Systems Biology, Harvard University, Boston, MA 02108, USA.
*Contact: igolding@princeton.edu (I.G.); ecox@princeton.edu (E.C.C.)
DOI 10.1016/j.cell.2005.09.031

SUMMARY

Protein levels have been shown to vary substantially between individual cells in clonal populations. In prokaryotes, the contribution to such fluctuations from the inherent randomness of gene expression has largely been attributed to having just a few transcripts of the corresponding mRNAs. By contrast, eukaryotic studies tend to emphasize chromatin remodeling and burst-like transcription. Here, we study single-cell transcription in *Escherichia coli* by measuring mRNA levels in individual living cells. The results directly demonstrate transcriptional bursting, similar to that indirectly inferred for eukaryotes. We also measure mRNA partitioning at cell division and correlate mRNA and protein levels in single cells. Partitioning is approximately binomial, and mRNA-protein correlations are weaker earlier in the cell cycle, where cell division has recently randomized the relative concentrations. Our methods further extend protein-based approaches by counting the integer-valued number of transcript with single-molecule resolution. This greatly facilitates kinetic interpretations in terms of the integer-valued random processes that produce the fluctuations.

INTRODUCTION

Gene expression involves a succession of probabilistic events: DNA continually undergoes conformational changes, repressors and transcription factors randomly bind and fall off their operators and promoters, and transcription and translation are complex at the levels of initiation, elongation, and termination (Kaern et al., 2005). Even in a hypothetically constant and homogeneous intracellular environment, this complexity would produce random fluctuations in the number of mRNAs and proteins per cell, constituting ''noise'' that cells must either exploit, learn to live with, or overcome using various noise-suppression mechanisms.

The last three decades have seen numerous probabilistic models of gene expression. Most fall into one of two categories. Some focus on how spontaneous small-number Poisson fluctuations in mRNA levels enslave the levels of their encoded proteins, possibly through bursts of translation (Berg, 1978; McAdams and Arkin, 1997; Rigney, 1979a, 1979b; Swain et al., 2002; Thattai and van Oudenaarden, 2001). Others instead focus on how mRNA fluctuations in turn are enslaved by random changes in gene activity and possible bursts of transcription (Blake et al., 2003; Kepler and Elston, 2001; Peccoud and Ycart, 1995; Raser and O'Shea, 2004; Sasai and Wolynes, 2003; Tapaswi et al., 1987).

The corresponding experimental interpretations have been similarly divided between these two categories. The first quantitative study, using a single GFP reporter in *Bacillus subtilis*, interpreted the results in terms of small-number mRNA fluctuations and translation bursts (Ozbudak et al., 2002). A second *E. coli* study used correlations between dual fluorescent reporters and similarly interpreted the inherent randomness of gene expression (termed ''intrinsic noise'') in terms of small-number mRNA fluctuations (Elowitz et al., 2002; Swain et al., 2002). In eukaryotes, on the other hand, the first single-reporter study in *Saccharomyces cerevisiae* suggested a substantial contribution from chromatin remodeling, producing quantal transcription bursts (Blake et al., 2003). A follow-up dual-reporter study (Raser and O'Shea, 2004) in *S. cerevisiae* greatly elaborated on these results and also suggested a substantial contribution from transcriptional bursting. Because chromatin remodeling is eukaryote specific, this has been suggested as a possible difference between these two domains of life (Blake et al., 2003).

A difficulty when analyzing the randomness of gene expression is that existing single-cell techniques only allow accurate quantitation of protein levels, while mRNA fluctuations are at best estimated qualitatively (Le et al., 2005; Tolker-Nielsen et al., 1998). Another difficulty is that single molecules of GFP are generally undetectable in vivo due to background fluorescence. With rare exceptions (Rosenfeld et al., 2005), fluorescence data therefore do not report the actual

number of molecules but rather a quantity that is roughly proportional to that number. This makes it harder to test stochastic models critically, where relative fluctuations depend on average numbers. Furthermore, the important molecules to count are the ones that contribute small-number fluctuations. If proteins are present in thousands of copies and protein fluctuations instead come from having low numbers of the corresponding mRNAs, then it is the mRNA that must be counted. Many studies have indeed attributed protein randomness to the low number of transcripts, but these studies were indirect, typically estimating protein distributions, altering experimental parameters, and using models to infer the source of fluctuations from the changes in the variance. This is in principal a valid approach and has produced many important insights, but a serious problem is that the same type of response in the variance tends to be consistent with very different kinetic explanations (Paulsson, 2004).

Here, we address transcriptional bursting in prokaryotes by directly counting the integer-valued number of stabilized mRNA transcripts in living *E. coli* cells, i.e., without "filtering" transcriptional fluctuations through RNA degradation, translation into proteins, proteolysis, and chromophore maturation. We also measure the physiological parameters of transcription with multiple methods and check all model assumptions quantitatively. The fluctuations in transcription are shown to scale as a Poisson process (variance proportional to average) but with substantially larger fluctuations. The fluctuations appear to come from transcriptional bursting, as suggested for eukaryotes. We also directly observe bursts from time-series data and show that the estimated distributions of both bursts and waiting times between events are perfectly consistent with expectations from the simplest models. Finally, by quantitatively comparing our findings to those of previous prokaryotic studies (Elowitz et al., 2002; Ozbudak et al., 2002) we show that the raw data sets are perfectly consistent and that the present results extend the conclusions by identifying the source of mRNA fluctuations.

In addition to the transcription results, we also study RNA partitioning at cell division and correlations between the levels of mRNAs and their encoded proteins. Partitioning is approximately binomial—as when individual transcripts segregate independently to identical daughters. The average number of proteins in a cell is shown to be proportional to the average number of mRNAs encoding that protein, something that is often assumed but rarely measured directly (for exceptions see Khodursky et al. [2000] and Lee et al. [2003]). In single cells, the correlations between mRNA and proteins were significantly weaker in more recently divided cells, consistent with the randomizing effect of segregation at cell division.

The genetic ingredients of our system are illustrated in Figure 1A. An MS2-GFP fusion protein was used to tag transcripts as they were made. The transcript target, produced from a single-copy F plasmid, consists of the coding region for a red fluorescence protein, mRFP1, followed by a tandem array of 96 MS2 binding sites. The two components were under the control of inducible promoters.

In a typical experiment, production of the fusion tag was first induced by adding anhydrotetracycline (aTc) to a growing culture. In experiments where arabinose was used, it was also preadded to obtain full induction of the *ara* system (Siegele and Hu, 1997). RNA transcripts were then induced with isopropyl-β-D-thiogalactopyranoside (IPTG), and samples were taken at different time points and imaged by fluorescence microscopy. Images of typical induced cells are shown in Figure 1B. Most cells contained green foci, each consisting of one or more tagged RNA molecules. Cells also expressed mRFP1. Figure 1C shows typical kinetics for the green (foci) and red (whole-cell) fluorescence levels, averaged over the cell population. RNA levels begin rising immediately after IPTG is added and approach a plateau after about 80 min. Protein levels rise more slowly, as expected: a stable protein should lag behind the mRNA, just as the mRNA lagged behind induction. The chromophore must also mature before fluorescence can be measured, adding at least a few minutes to the observed protein response (Campbell et al., 2002).

At very low transcript levels, each mRNA molecule is detectable as a single focus occupied by 50–100 MS2-GFP molecules (Golding and Cox, 2004), but at higher levels what appears as a single focus may consist of several transcripts. Our way of estimating the number of mRNA molecules in the cell is to count the total number of bound MS2-GFP proteins. We therefore measured the total photon flux of all green foci above the cell background (see Experimental Procedures). This value was then normalized by the intensity of a single tagged RNA molecule—equal to the first peak in the intensity histogram (Figure 1D)—to calculate the number of transcripts per cell. The normalized intensity histogram for the number of transcripts per cell consists of a series of discrete peaks, each corresponding to the integer-valued number of individual mRNA molecules in the cell. This result is central to our approach: when estimating an integer-valued distribution of numbers of molecules using a continuous quantity like fluorescence, such well-separated peaks are an indication of the measurement's fidelity.

RESULTS

Dynamic Range and Accuracy of the Measurements

We have optimized the MS2-GFP induction level to enable robust mRNA detection and measurement. This means that we must have sufficient MS2-GFP to saturate all RNA targets, but not too much MS2-GFP, which would create too high a fluorescent background level in the cell. We have found that there exists a large "dynamic range" of MS2-GFP (obtained by inducing the Tet controlled system for 0.5–2 hr at maximum induction), within which the above conditions are fulfilled. Based on fluorescence measurements (6 different experiments, >2700 cells), each cell contains $\sim 10^4$ MS2-GFP molecules (approximately ~ 10 μM) in this induction range. Of these molecules, typically only 3%–4% are bound to RNA targets, with a maximum fraction of ~10% at the highest RNA levels (>10 transcripts per cell). These percentages are consistent with the fact that the MS2-GFP gene is located on a ColE1 plasmid, with a copy-number >50 times higher than the plasmid carrying the RNA-coding target, and expressed from a stronger promoter (Lutz and Bujard, 1997).

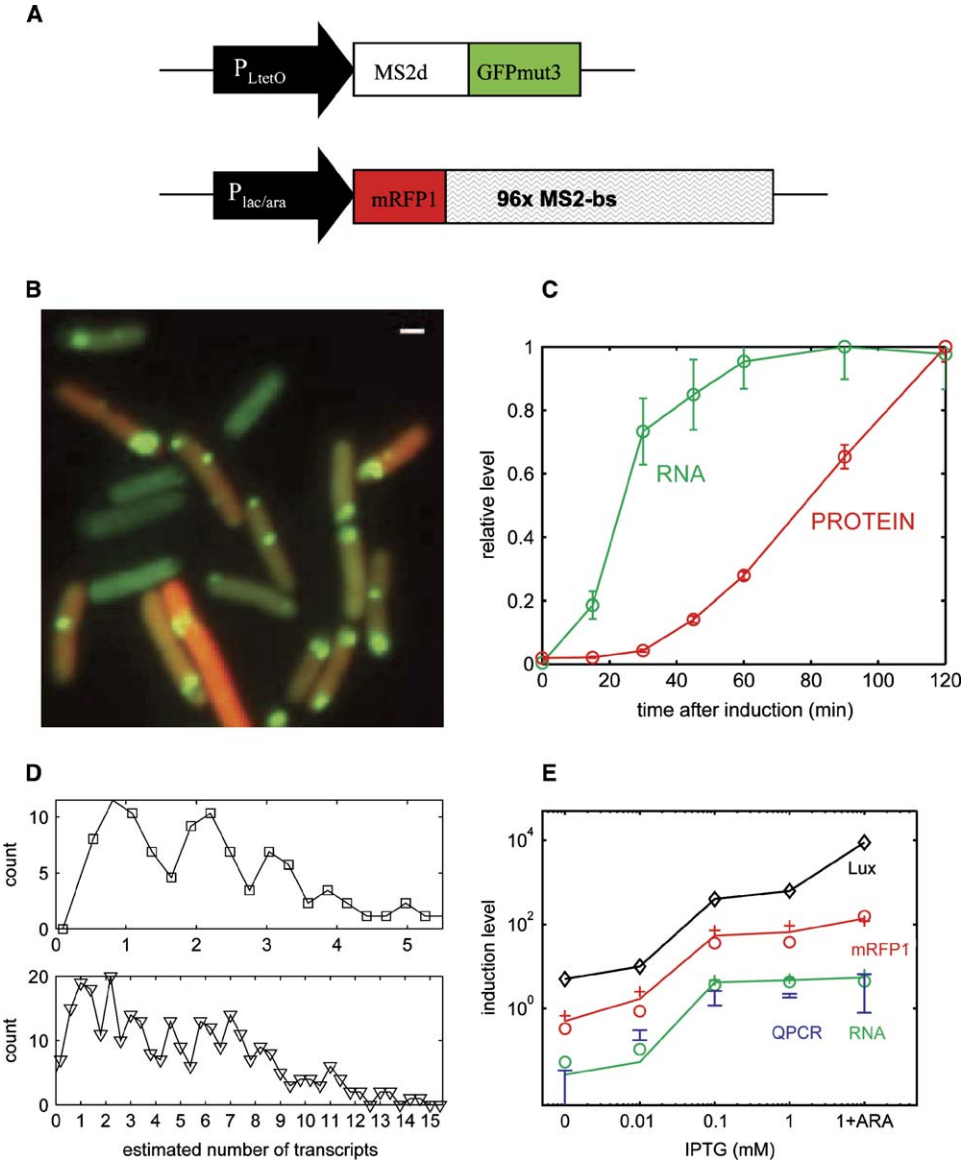

Figure 1. Measuring mRNA Levels in Living Cells

(A) Genetic components of the detection system. The tagging protein consists of a fused dimer of MS2 coat protein fused to GFP. Protein production is regulated by the P_{LtetO} promoter (Lutz and Bujard, 1997), and inducible by anhydrotetracycline (aTc). This construct is on a ColE1 plasmid. The RNA target consists of the coding region for mRFP1, a monomeric red fluorescence protein (Campbell et al., 2002), followed by a tandem array of 96 MS2 binding sites. This message is under the control of a $P_{lac/ara}$ promoter (Lutz and Bujard, 1997), which is repressed by LacI and activated by AraC, therefore inducible by isopropylthio-β-D-galactoside (IPTG) and arabinose. This construct is on an F plasmid, with a single copy per bacterial chromosome. Both plasmids were cotransformed into *E. coli* DH5α-PRO, a constitutive producer of LacR and TetR repressors. For construction of the components, see Experimental Procedures.

(B) Detection of mRNA and protein in living cells. The picture is a false-colored overlay of the green and red channels. Scale bar, 1 μm.

(C) Kinetics of mRNA (green) and protein (red) levels after addition of IPTG. Cells were grown and induced as described in Experimental Procedures. At different times after induction, ~100 cells were imaged. The images were then automatically processed (see Experimental Procedures) to identify individual cells and within them the location of green particles. The average green signal ($\langle I_G \rangle$) is the average over all cells at one time point of the total photon flux from all green foci in the cell, from which the cell background green fluorescence was subtracted. The red signal ($\langle I_R \rangle$) is the average over all cells at one time point of total cell red fluorescence. Bars denote standard error of the sample over the population.

(D) Distribution of estimated mRNA copy numbers among different cells in two typical samples. The estimated copy number n is equal to I_G normalized by the intensity of a single tagged mRNA molecule.

(E) Gene expression levels at various levels of induction, obtained by varying the levels of IPTG and arabinose. Green: estimation of mRNA levels (molecules/cell) at steady state, using our fluorescence-based method. Markers (O, +) are results of two separate experiments (>300 cells in each); lines connect the averages. Blue: mRNA levels measured by QPCR. Shown are the average and standard error of message levels in two separate experiments. Red: red fluorescence levels of the induced cells in arbitrary units. Data are from the same experiments as the estimated mRNA levels (same markers). Black: luciferase levels measured from the $P_{lac/ara}$ promoter (in arbitrary units). Data from Lutz and Bujard [1997].

Because the dissociation constant between MS2 coat protein and our version of the binding site is in the ~nM range (Johansson et al., 1998), all of the target RNAs are expected to be saturated by the MS2-GFP pool, i.e., the occupancy of MS2 binding sites is expected to be close to 100%. In agreement with this view, population measurements show that cells with above-median RNA levels exhibit only a slightly lower (5%–10% difference) level of unbound green fluorescence compared to cells with below-median RNA levels. At the single-cell level, the appearance of a new mRNA is usually not accompanied by a detectable decrease in cell background fluorescence.

To check that the estimation of mRNA levels is consistent with other methods, we compared single-cell measurements to three other indicators of gene expression: quantitative real-time PCR (QPCR), levels of the proteins encoded by the RNA transcripts, and luciferase levels measured from the same promoter as reported in the literature (Lutz and Bujard, 1997) (Figure 1E). Fluorescence measurements are in good agreement with the other indicators over most of the induction range. The agreement with QPCR further strengthens our belief that absolute levels of message copy number have been reliably estimated.

In addition to the integer-valued peaks in the photon-flux histograms and the comparisons with standard measures of gene activity (QPCR for RNA, fluorescence and luciferase for protein), a series of additional experimental controls (detailed below) points to the fidelity of our measurements: (1) the observed statistics of RNA partitioning is approximately Binomial up to at least n = 15 (see Figure 3D). A similar protein experiment (Rosenfeld et al., 2005) used such statistics to estimate protein numbers, even without counting the number of molecules. (2) The adjustment to steady state follows a first-order model (Figure 2A). (3) We observe proportionality between RNA and protein levels (Figure 4) over a broad range of induction. These points are discussed in more detail in the following sections.

Another possible concern is whether the long array of 96 MS2 binding sites (96 bs) hinders proper transcription and translation. To examine that, we measured expression levels (as indicated by red fluorescence of the individual cells) from two modified constructs, both having the same genetic background (pTRUEBLUE-BAC2 plasmid with $P_{lac/ara}$ promoter) as our mRFP1 + 96 bs construct: (1) a plasmid carrying the mRFP1 gene only, without the MS2 binding sites array. In this case, the protein levels obtained are almost indistinguishable from those of the original construct: [R]/[R + 96 bs] = 0.82 ± 0.28 (two experiments, 310 cells; where [ ] denotes mRFP1 fluorescence level). (2) A plasmid in which the mRFP1 gene is located downstream of the 96bs array, instead of upstream as in the original construct—in this case, there is a slight repression of the expression level (3.0 ± 0.3-fold; 3 experiments, 240 cells). Considering the length of the transcript on the 5′ side of the gene (~4 kb), this is a small polarity effect (Li and Altman, 2004).

These results are in agreement with additional data pointing at the normal behavior of the transcript: (1) we measured in two different ways the kinetics of mRNA chain elongation in the GFP-tagged (=MS2 bs array) portion of the transcript. This was done by measuring the increase in fluorescent signal (Figure 3A) and by measuring the physical elongation of the transcript (Golding and Cox, 2004). Both methods reveal a very similar chain elongation rate, close to the rates estimated from in vivo population studies (Ryals et al., 1982) and from in vitro single-molecule studies (Shaevitz et al., 2003). This result implies that the 96 bs array behaves as a normal transcript with regards to its transcription kinetics. (2) As described above, we also examined the ''dose response'' of the two coding regions of our transcript: the mRFP1 gene (as measured by cell red fluorescence) and the 96 bs array (as measured by localized green fluorescence). As shown in Figure 1E, their behavior is very similar, again indicating that the 96-mer does not seriously perturb the dynamics of transcription.

Average Transcriptional Response

Before analyzing statistics in single cells, it is helpful to demonstrate that the average dynamics behave as expected. Figure 2A shows the average number of transcripts per cell $\langle n \rangle$ as a function of the time after induction t. Under full induction, $\langle n(t) \rangle$ starts at $\langle n \rangle << 1$ at $t = 0$ and approaches a steady-state value of $\langle n \rangle \approx 10$ after approximately 100 min. This level is then maintained for many cell generations. To interpret the average induction curve, we assumed a constant rate of production k_1 and first-order elimination with rate constant k_2:

$$\frac{d}{dt}\langle n \rangle = k_1 - k_2 \langle n \rangle. \quad (1)$$

Solving Equation 1 yields:

$$\langle n(t) \rangle = \frac{k_1}{k_2}\left(1 - e^{-k_2 t}\right) \Rightarrow \frac{\langle n(\infty) \rangle - \langle n(t) \rangle}{\langle n(\infty) \rangle - \langle n(0) \rangle} = e^{-k_2 t}. \quad (2)$$

The second formulation in Equation 2 shows that the relative deviation from steady state decreases exponentially and independently of k_1, i.e., the dynamic response is set by the elimination rate constant, not by the synthesis rate constant. Parameter k_2 can thus be determined independently of k_1. Figure 2A compares the experimental response with the theoretical curve defined by Equation 2, showing that indeed the data is well characterized by a single exponential approach to steady state. For most mRNAs, elimination is dominated by degradation (Bernstein et al., 2002), while elimination through cell growth and division has a marginal effect. In our system, however, the binding of MS2-GFP, with a dissociation constant in the ~nM range and corresponding dissociation times of ~hours, (Johansson et al., 1998), increases the transcript lifetime. When individual growing cells are followed, the mRNAs are ''diluted away'' when cells divide (see Figure 3A). In addition, when individual foci are followed for many generations, they exhibit a slow decrease in intensity (rate < 1 hr^{-1}), consistent with the message slowly being ''chewed up'' and GFP molecules dissociating. Thus, cell division dominates the negative term in Equation 1. For consistency, the value of k_2 should thus equal $ln(2)/\tau_g$, where τ_g is the cell generation time. Indeed, the curve describing the approach to the steady state (Figure 2A, inset) is in good agreement with the value of k_2

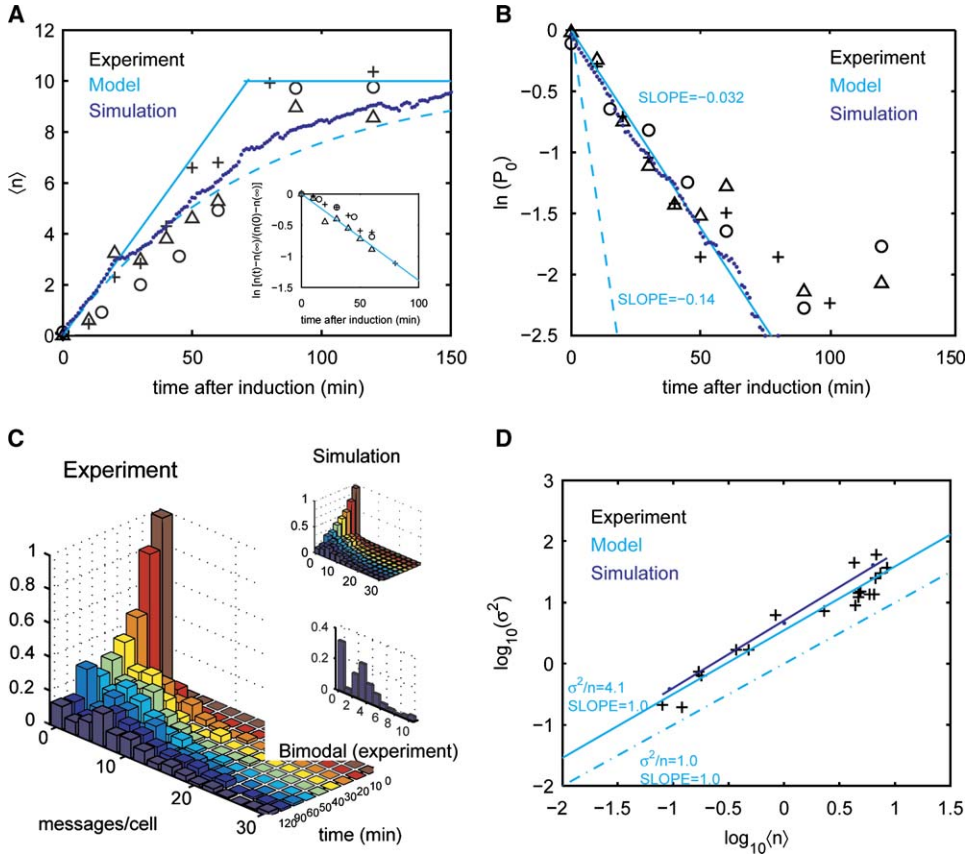

Figure 2. Induction Kinetics

(A) Estimated average number of transcripts per cell $\langle n \rangle$, as a function of time after induction t. Fifty to one hundred cells were imaged at each time point and the number of tagged mRNAs in each cell was estimated (see Experimental Procedures). $\langle n \rangle$ is averaged over all cells at a given time. Symbols (+, o, Δ) are results of three different experiments. Dashed line (cyan) is the prediction of the first order model (Equation 2), with parameters $k_1 = 0.14\ \text{min}^{-1}$, $k_2 = ln(2)/50\ \text{min}^{-1}$. Solid line (cyan) consists of the two asymptotes of the theoretical expression $n(t) = k_1 t$ (short times) and $n(t) = k_1/k_2$ (long times). Dotted blue line—the results of a stochastic simulation of the bursting message model (see text). Inset: relative deviation from steady state, as a function of time after induction. Symbols are experimental data. Line (cyan) is the prediction of the first order model (Equation 2).

(B) Fraction of cells having no tagged RNA (P_0) as a function of time after induction t. Data (+, o, Δ) are from the experiments in (A). Also shown (cyan, dashed line) is the theoretical prediction of the first-order transcription model $P_0(t) = e^{-k_1 t}$ (Equation 3), with the same parameters used in (A). The actual decline is about four times slower, with a rate of approximately 0.032 min^{-1} (cyan, solid line). Blue: a stochastic simulation of the bursting mRNA model (see text).

(C) Histograms of mRNA copy numbers in the cell at various times after induction. Data is from one of the experiments in (A). Starting from an almost uniform population, with most cells having no messages at $t = 0$, the average copy number increases with time, as does the width of the distribution. Top inset: histogram resulting from simulation of the mRNA bursting model (see text). Bottom inset: histogram of mRNA copy numbers at $t = 30$ min after induction. In this experiment, cells were not preinduced with arabinose. Instead, 0.1% arabinose was added together with IPTG at $t = 0$. This induction procedure leads to a strong bimodal distribution of mRNA in the population, due to the autoregulatory nature of the *ara* system (Siegele and Hu, 1997).

(D) Variance (σ^2) versus average ($\langle n \rangle$) of mRNA copy number. The data (+) are from four different experiments, each at multiple induction levels. Dashed line (cyan) is the theoretical prediction based on a Poisson model, with $\sigma^2 = \langle n \rangle$. Solid line (cyan) is a least-mean-square fit of the data to a first-order polynomial. This fit yields a slope of 1.0 (in log-log), implying proportionality of σ^2 to $\langle n \rangle$. The average of $\sigma^2/\langle n \rangle$ is 4.1. Also shown (blue spots and least-mean-square fit) are the results of the mRNA-bursting simulation (see text) run at various bursting rates (the parameter k_1, corresponding to the experimental induction levels), using the same average burst of 4.

expected from our independently measured generation time: $\tau_g \approx 50$ min, k_2 (measured) = 0.014 ± 0.002 min^{-1}. We note that the stability of the transcript is highly advantageous for our purposes and allows us to study the randomness of transcription without convolving the results with the randomness of RNA degradation.

Once the value of k_2 has been determined, a value of $k_1 = 0.14 \pm 0.02\ \text{min}^{-1}$ follows immediately from the level of the steady state, $\langle n(\infty) \rangle = k_1/k_2$. To check that the same value of k_1 accounts for the entire postinduction period and not just the steady state, we independently determined its value from the initial time points where Equations 1 and 2 simplify to $d\langle n \rangle/dt \approx k_1$ and $\langle n(t) \rangle \approx k_1 t$, that is, where so few transcripts have accumulated that elimination can be ignored. This produced a consistent value of $k_1 \approx 0.10 \pm 0.02\ \text{min}^{-1}$.

Single-Cell Transcriptional Response—Testing the Poisson Hypothesis

The simplest microscopic mechanism that produces a constant average rate of synthesis is the Poisson process, with

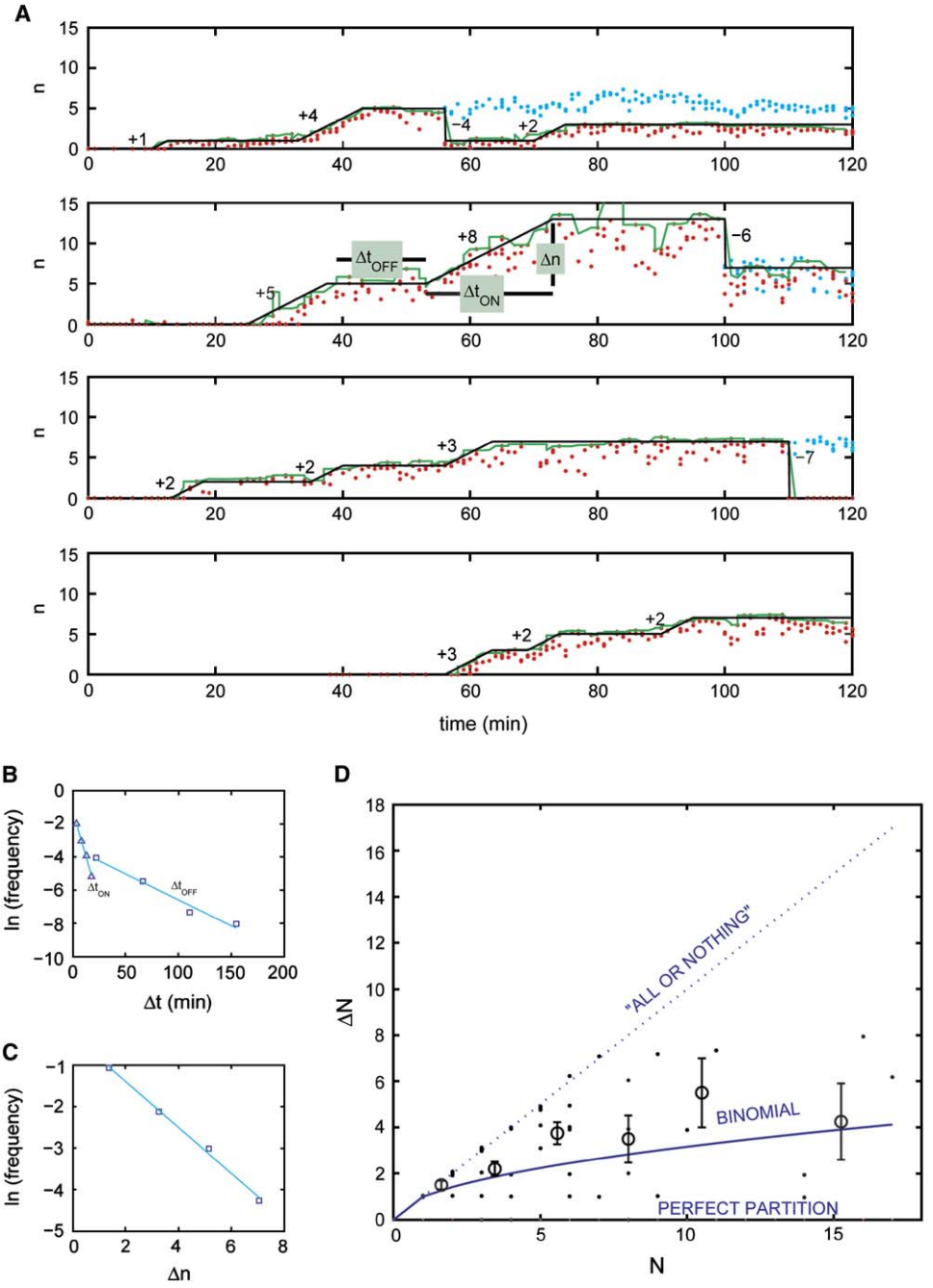

Figure 3. Induction Kinetics in Individual Cells

(A) Estimated number of transcripts per cell n, as a function of time t, in typical cells. Cells were grown and induced for MS2-GFP, and at time $t = 0$ a few μl of cell culture was placed under a thin LB-agarose slab with IPTG (1 mM) and aTc (100 ng/ml). Fluorescent images were taken for 2 hr, at 2 frames/min. Red dots, raw data. Green line, data smoothed by taking the maximum value in a six-sample running window. Black lines are fit by eye to a piecewise linear function. This fit describes periods of transcriptional inactivity (constant n), separated by transcriptional events, in which RNA is produced at a rate of 1 transcript per 2.5 min. This rate corresponds to a chain elongation rate of ~25 nucleotides/sec, in close agreement with our earlier measurements (Golding and Cox, 2004), as well as with the known rate of chain elongation in *E. coli* at 22ºC (Mathews et al., 2000; Ryals et al., 1982). Cyan spots are measurements made in the sister cell after cell division, demonstrating the randomness of RNA partitioning (D). Also marked in the figures are the measured jumps Δn in RNA level following transcription, as well as negative changes in n following cell division.

(B) Distribution of inactivity periods (Δt_{OFF}, squares) and activity periods (Δt_{ON}, triangles). Data is from 20 cells and 77 transcription events. Line is a fit to an exponential distribution. Mean Δt_{OFF} is ≈37 min; mean Δt_{ON} is ≈ 6 min. Note that Δt_{ON} is equal to Δn times the duration of transcribing 1 message, 2.5 min—see below.

(C) Distribution of RNA "jumps" (Δn). Squares are data, cyan line is a fit to an exponential distribution. Same data set as (B). The mean Δn is ≈ 2.2.

constant probability per unit time of making a transcript. The probability for zero events then decreases exponentially with time, with the same rate constant that governs the average synthesis. If transcription truly were Poissonian, the fraction of cells where zero transcription events have occurred at time t after induction, $P_0(t)$, should follow:

$$P_0(t) = e^{-k_1 t}. \quad (3)$$

Because we showed above that $k_1 \gg k_2$, the effect of transcript elimination can initially be ignored. At short times t after induction, $P_0(t)$ can thus be estimated from the fraction of cells that contain zero transcripts. Figure 2B is the experimental estimate of $P_0(t)$ compared to the theoretical prediction, using the value of k_1 that was determined from the average dynamics above. This shows that $P_0(t)$ indeed decreases exponentially, at least up to $t \sim \tau_g$ where the test is expected to break down. However, the exponential decay rate is $0.032 \pm 0.005\ \text{min}^{-1}$, which is about four times (4.4 ± 1.4) smaller than the estimated value of k_1 above. The underlying stochastic process is therefore not Poissonian, despite the fact that the first event occurs after an exponentially distributed lag.

By counting the number of molecules per cell, the cell-to-cell heterogeneity in transcript levels can also be tested against the Poisson hypothesis that the variance equals the average (van Kampen, 1992), $\sigma^2 = \langle n \rangle$. Here, the cells grow and divide, and individual cells are sampled from an asynchronous population. Both complications can easily be built into the model, but to minimize complexity and reduce the number of parameters we instead normalized the measured numbers by the individual cell sizes (Elowitz et al., 2002). The observed variance was then compared to model predictions assuming that elimination at cell division can be approximated by first-order exponential deaths (Thattai and van Oudenaarden, 2001), producing $\sigma^2 \approx \langle n \rangle$ if the synthesis is truly Poissonian. Figure 2C is a histogram of measured mRNA numbers at various times after induction, and Figure 2D shows the variance at steady-state as a function of the average at different levels of induction. Over a 100-fold range, the variance is almost perfectly proportional to the average, as expected from a Poisson distribution. But the proportionality constant is again four times higher than expected ($\sigma^2 / \langle n \rangle = 4.1 \pm 0.5$).

The linear-average dynamics with constant parameters, the exponentially distributed waiting times, and the proportionality between the variance and the average, are precisely the behaviors expected of Poisson processes and Poisson distributions. But by counting the individual molecules, we see that the actual numbers are off by a factor ~4 from the Poisson expectation. To address this issue, we now suggest a modified Poisson process, test its assumptions independently, and show that it indeed generates the statistics observed above.

Bursts of Transcription

To explain the observed heterogeneity, we return to previous models of random gene activation-inactivation (Kepler and Elston, 2001; Peccoud and Ycart, 1995; Raser and O'Shea, 2004; Sasai and Wolynes, 2003). The most common kinetic assumptions are that genes in the OFF state switch ON with a constant probability, and that genes in the ON state either switch OFF or make a transcript with constant probability. In mathematical terms, activity is assumed to switch at exponentially distributed intervals, as in a "random telegraph process" (Gardiner, 2004), and transcription is assumed to be Poissonian when the genes are ON. The number of transcripts made in the ON periods will then vary randomly. The combined effect of the two sources of randomness—the exponential duration and the Poissonian synthesis—is that a geometrically distributed number of molecules are transcribed in each ON period (Berg, 1978). The geometric distribution is essentially an integer-valued version of the exponential distribution and describes the number of heads before the first tail when tossing an unfair coin. In the present case, it can be calculated by convoluting the Poisson process over exponentially distributed times or simply by recognizing that the cell effectively tosses a coin to decide whether to make another transcript (tails) or turn OFF the gene (heads). With a single copy of the gene, a random period of inactivity (OFF) is thus followed by a random period of activity (ON). If long OFF periods are followed by intense ON periods that produce a significant number of transcripts, transcription is said to occur in "bursts."

To directly demonstrate the bursts and to measure the relevant physiological parameters, we followed transcription of individual messages over time and calculated the statistics of bursts and switch-time intervals. Exponentially growing cells expressing MS2-GFP were placed between a coverslip and a thin nutrient agarose slab containing the required inducers (IPTG and aTc) at 22ºC where they grew and divided normally (see Experimental Procedures). We then followed RNA levels in individual cells as they increased during the cell cycle and abruptly dropped at cell division (Figure 3A). The cells exhibited a discrete distribution of measured RNA levels (see lower histogram in Figure 1D), corresponding to mRNA copy number. No increase in RNA levels was detected when cells were grown without IPTG (data not shown). Under these conditions, we were also able to show that the rate of decrease in the intensity of individual foci was very low ($<1\ \text{hr}^{-1}$), in accord with our previous observation that the tagged transcripts are stable.

Figure 3A shows that transcription is characterized by periods of inactivity Δt_{OFF}, followed by periods of activity Δt_{ON}, each producing a random jump of size Δn in the RNA level. Figure 3B shows that the distribution of both Δt_{ON} and Δt_{OFF} are accurately described by exponentials, as expected from the simplest models. The averages are $\langle \Delta t_{ON} \rangle \approx 6$ min and

(D) Statistics of RNA partitioning at cell division. Shown is the difference in RNA molecule number inherited by the two daughter cells ΔN versus the number of molecules in the mother cell N. Spots are data from 54 cell divisions. Circles are binned data and bars denote standard error. The blue solid line describes the binomial expectation $\langle \Delta N \rangle \approx \sqrt{N}$. The dotted line is the limiting case where all RNA molecules end up in one daughter cell ($\langle \Delta N \rangle = N$). At the other extreme of perfect partitioning, $\langle \Delta N \rangle = 0$. The data appears to be close to the binomial expectation.

$\langle \Delta t_{OFF} \rangle \approx 37$ min (20 cells, >77 transcription events), so transcription indeed seems to occur in intense periods, as can also be seen directly in the time series (Figure 3A). Figure 3C shows the distribution of Δn from the same data set, again very well approximated by the predicted geometric or exponential behavior. The statistics are consistent with a bursting model where $\Delta n > 1$ is the most likely event.

Because effective ON periods are relatively short, the ON-OFF switching and subsequent transcription can be condensed approximately into a Poisson process where each event adds a geometrically distributed number of molecules, i.e., quantal burst of mRNA appearance. This can then be used to further simplify the mathematical models and explain our previous findings. First, the rate constant for the decrease of $P_0(t)$ in Equation 3 is simply $k_1^0 = k_1 \langle \Delta n \rangle^{-1}$, i.e., the observed exponential decrease is expected but with a $\langle \Delta n \rangle$-times lower rate compared to the Poisson case. Second, the variance follows $\sigma^2/\langle n \rangle = \langle \Delta n \rangle$(using the formal analysis in Thattai and van Oudenaarden [2001]). Thus, the observed proportionality to the average is expected, but with a $\langle \Delta n \rangle$-times higher proportionality constant. The observed bursting thus not only explains both results, it also explains why both variables differ from the Poissonian expectation by the same factor. The 4-fold effect observed in the 37ºC statistics experiments (Figure 2) is not identical to the 2-3-fold effect predicted from the burst measurements that were run at 22ºC (Figure 3) (due to microscopy conditions). But the numbers are close and, more importantly, the experiments confirm the shape of the distributions—that is to say, the types of stochastic assumptions we have made.

From the measurements above, we can also estimate the randomness of RNA partitioning at cell division—how many RNA molecules end up in each of the daughter cells? Most theoretical models have assumed that the RNA molecules segregate independently to identical daughters. On this hypothesis, RNA partitioning will exhibit binomial statistics, characterized by the relation $\langle \Delta N \rangle \approx \sqrt{N}$, where $\langle \Delta N \rangle$ is the average difference in molecule numbers inherited by the two daughter cells and N is the number of molecules in the mother cell. For example, if the mother has ten copies ($N = 10$) and the two daughters receive three and seven each, then $\Delta N = 7 - 3 = 4$. As can be seen in Figure 3D, the data strongly suggest that partition fits the binomial expectation.

To illustrate how these characteristic dynamics can be obtained in growing and dividing cells, we devised a computer simulation for a population of 500 cells. The only assumptions were that each cell has a constant probability per unit time of generating a geometrically distributed burst of transcripts ($\Delta n = 4$), that cells grow from normalized size 1 to 2 in one generation (50 min) and then divide, and that transcripts segregate independently to the two identical daughter cells (binomial partitioning). Simulated data using the Gillespie algorithm (Gillespie, 1977) was collected for 150 min, corresponding to three cell generations. The numerical model reproduces all the analytically expected and experimentally observed main features noted above, including the shape of the copy-number histogram. This is summarized in Figures 2A–2D.

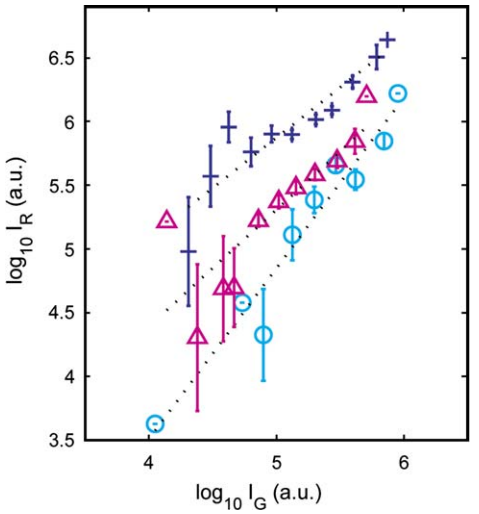

Figure 4. Quantifying Translation

Average green fluorescence levels of mRNA foci (I_G) versus red fluorescence levels (I_R) in three typical experiments. Cells were induced at a range of induction levels (0–1 mM IPTG, 0%–0.1% arabinose). The cultures were maintained in exponential growth for 5 hr by constant dilution into fresh medium. Different markers (+, o, Δ) denote different experiments. Bars are standard errors of the average. Dotted lines are least-mean-square linear fits. The normalized correlation coefficients for I_G and I_R (log scale) in these experiments are in the range 0.85–0.98, and the least-mean-square fitted slope for $log_{10}(I_R)$ versus $log_{10}(I_G)$ is 1.0 ± 0.17. In RNA constructs containing the MS2 binding sites but no mRFP1 gene, no red fluorescence was detected above background (data not shown). Two hundred to five hundred cells were imaged and analyzed in each experiment.

Correlating mRNA and Protein Levels

The protein product of our tagged mRNA is a red fluorescent protein, mRFP1. For the average levels in our $P_{lac/ara}$ system, we find that the steady-state protein level is directly proportional to the mRNA level (see Figure 4). This proportionality is commonly assumed but is not self-evident because it implies that transcription and translation are decoupled (Gowrishankar and Harinarayanan, 2004). Numerous nonlinear couplings could be imagined, such as nonsense polarity (Yanofsky and Ito, 1966) and saturating ribosomes or RNases at high mRNA levels.

By measuring the levels in individual cells, we can also examine correlations between the two components. One striking observation is that the correlation between mRNA and protein is much weaker in more recently divided cells. Grouping the cells into larger-than-median and smaller-than-median sizes, the mRNA-protein correlation coefficient for the large cells was 0.23 ± 0.05, compared with a vanishingly small value (<0.04) for the small cells (data from four experiments, >600 cells). We believe that this is due to the randomizing effect of cell division: because the cells just prior to division have relatively large numbers of proteins, each daughter receives close to 50% of the total at cell division. But the number of transcripts is so low that random segregation will introduce large relative differences between the two cells, as explicitly demonstrated in Figure 3D. A strong correlation at the end of the cell cycle—when the transcripts have been producing proteins for

some time—is then effectively forgotten. This effect should be stronger for mRNAs at lower numbers or with longer lifetimes and can be further pronounced if individual transcripts tend to cosegregate due to cell-localization effects.

Incorporating protein production as a Poisson process and partition with binomial statistics into our RNA bursting simulation produces the same overall result: older cells exhibit a stronger protein/RNA correlation than younger ones. Only a qualitative fit can be expected without making exact assumptions about chromosome replication, the randomness of cell division times, and other sources of protein randomness, the details of which are unknown in our system.

Finally, we can obtain an estimate for the average number of mRFP1 proteins produced by each mRNA molecule in a cell lifetime. For this purpose, we estimate $p = \langle m/n \rangle$, where m and n are the numbers of protein and mRNA molecules per cell in a population that has reached steady state. In order to obtain p, we write (for each cell):

$$I_G = nNf_{GFP},$$

$$I_R = mf_{RFP}.$$

These equations describe the fact that the measured intensity of green fluorescent particles in the cell (I_G) is the result of the number of RNA molecules (n), each tagged with N GFP molecules ($N \sim 50$–100), where a single GFP has a photon flux f_{GFP}. Similarly, red fluorescence (I_R) is proportional to the number of mRFP1 proteins in the cell (m), with the proportionality coefficient determined by the flux of each one, f_{RFP}. From the experiments described in the text (and see Figure 4), we obtain $\langle I_R/I_G \rangle = 3.1 \pm 0.2$.

To estimate the flux ratio f_{RFP}/f_{GFP}, which is a function of the molecules themselves, as well as of our optical system, we used a pair of constructs which differ only in their fluorescent protein. The constructs are a fusion protein of MS2 with either GFP or mRFP1 under control of the P_{LtetO} promoter in a ColE1 plasmid. Two sets of measurements were performed: the first by inducing the fusion protein alone and measuring the fluorescence levels in the cells and the second by inducing the fusion protein in the presence of the target mRNA and measuring the fluorescent intensity of the tagged transcripts (either green or red). These measurements yielded $f_{RFP}/f_{GFP} = 3 \pm 1$. Using these values, we obtain

$$\langle p \rangle = \langle m/n \rangle = N^* \, (f_{GFP}/f_{RFP})^* \, (\langle I_R/I_G \rangle) \approx 60\text{–}110.$$

This value compares well with the estimate made in Kennell and Riezman (1977) for the *lac* operon (about 5–40), taking into account the longer lifetime of our tagged RNA. The estimated number of mRFP1 proteins in a fully induced state ($m \sim 1000$) also agrees with the original estimates for this promoter, based on measured luciferase activity (Lutz and Bujard, 1997).

DISCUSSION

Gene expression is directly involved in almost every life process, but surprisingly little is known about the kinetic mechanisms in the individual cells where they operate. Large cellular fluctuations have been predicted (Delbruck, 1940; Schrodinger, 1944) and observed (Benzer, 1953; Novick and Weiner, 1957) for half a century, yet single-cell analyses are still severely restricted by the available methods. For example, even though most studies of stochastic cell processes have emphasized that protein fluctuations are caused by fluctuations in the corresponding mRNAs, all measurements have been done on protein levels. With one recent exception (Rosenfeld et al., 2005), they have also been constrained to snapshots across populations rather than time series in individual cells. Finally, because total GFP fluorescence is only approximately proportional to the number of GFP molecules, very far from single-molecule resolution, it has been difficult to compare critically the data to probabilistic models where absolute numbers determine relative fluctuations. These difficulties have been partially overcome by an array of creative approaches (Blake et al., 2003; Elowitz et al., 2002; Ozbudak et al., 2002; Raser and O'Shea, 2004; Rosenfeld et al., 2005; Thattai and van Oudenaarden, 2001) and have then been used to address various biological questions.

In the current work, we used in vivo tagging of mRNA to monitor transcript numbers in living *E. coli* cells, with single-molecule resolution. After demonstrating the fidelity and dynamic range of our method, we used it to characterize transcription kinetics in individual cells. We found that transcription occurs in quantal bursts, even in fully induced cells; that the burst sizes are geometrically distributed; and that the time intervals between bursts are exponentially distributed. All these features are expected from a simple gene activation/inactivation model. The bursting behavior observed in single-cell induction kinetics also explains several different statistical properties of the population data.

To show bursts in transcription, three separate methods were used. We note that although our mRNA-counting method has proven reliable over a large range of levels, none of the main results of this study actually rely on accuracy at high numbers. The distributions for waiting times and numbers of molecules both scaled as if transcription were Poissonian, but with a 4-fold deviation in the proportionality constant in both cases—a number that is large compared to the estimated experimental error. These experiments were done at low transcript averages where the method is most reliable: The first-event measurement separates zero from one copy, and the distribution experiment was done from 0.08–8 copies on average. The third method used time series. The single-cell data shown in Figure 3 reveal many clear burst events followed by longer periods of no transcription. Importantly, the estimated distributions for the bursts and the waiting time between bursts are the exponential (or geometric) shapes expected from theory. This observation is not necessary to make our claim, but it does lend further credence to the on-off model.

Origins of RNA Bursting

Chromatin remodeling has been suggested to cause transcription bursts in eukaryotic studies (Kaern et al., 2005). In both pro- and eukaryotes, the same pulsatile effect might also result from other mechanisms: activators (in our case AraC) or repressors (in our case LacI) binding and falling off their binding sites, DNA undergoing conformational changes

such that the polymerase has access for brief periods only (Guptasarma, 1995; Guptasarma, 1996), or transcription reinitiation due to retention of sigma factor during the elongation process (Bar-Nahum and Nudler, 2001; Dieci and Sentenac, 2003). In relation to this last possibility, it is interesting to note that in our single-cell time series data (Figure 3A), the duration of a transcription event seems to be proportional to the number of transcripts made during that period, possibly implying that transcripts are made consecutively (one at a time), rather than in parallel. We also point to the possible relation between our findings and the rarely referred-to results of Baker and Yanofsky (1968), Imamoto (1968), and Contesse (Beckwith et al., 1970; Contesse et al., 1969) describing periodic transcription initiation in the *lac* and *trp* operons. Bursting could in principle also arise during chain elongation, for example due to pausing of RNA polymerase during transcription (Artsimovitch and Landick, 2000; Shundrovsky et al., 2004) and the subsequent queuing of adjacent enzymes transcribing the same template (Bremer and Ehrenberg, 1995; Epshtein and Nudler, 2003; Foe, 1978).

One may ask to what degree our results are general and to what degree they depend on the specific details of promoter and transcript used in this work. We chose the synthetic $P_{lac/ara}$ promoter because it is so well characterized and because it has the same logical structure as the *lac* promoter, with the hybrid workings of an activator and a repressor. As in many previous single-cell studies, we thus follow in the recent tradition of synthetic biology to facilitate the study of a particular process—in this case transcription—by minimizing effects of other cellular control circuits. To generalize the results, we constructed a reporter system for a second promoter, the P_{RM} promoter of bacteriophage λ. Despite the very different regulatory characteristics of this promoter, it too exhibits transcriptional bursting with a similar mean burst size (see Supplementary Data available with this article online).

As for the unique transcript used in our work, the length of our transcript (~4.5 kb) is of the order of typical polycistronic operons (e.g., *lac* and *trp*) prevalent in the bacterial genome (Neidhardt, 1996). We cannot rule out the possibility that the transcript length or the multiple MS2 recognition sites amplify the pausing effect relative to an indigenous transcript by affecting RNA polymerase processivity. We note, however, that hairpin formation by itself is not sufficient to signal a pause in elongation (Uptain et al., 1997). As described above, multiple measurements strongly suggest that transcription in our system behaves normally and hence that our observations are intrinsic to transcription. Moreover, because we see the same general features with a 48 binding site array (in the case of the λ P_{RM} reporter), we can have additional confidence in our central conclusions.

Additional discussion is included in the Supplemental Data: Comparison with Previous Models and Experiments; Intrinsic and Extrinsic Noise.

EXPERIMENTAL PROCEDURES

Genetic Constructs

For the construction of the MS2-GFP fusion and the 96 binding site array, see (Golding and Cox, 2004).

Construction of the RNA Target

A promoter-less version of pTRUEBLUE-BAC2 (Genomics One International, Buffalo, NY) was created by amplifying the plasmid sequence minus the original P_{lac} region, with primers containing an AatII restriction site. The PCR product was then digested with AatII, religated, and cloned into *E. coli* strain DH5α-PRO. Promoter $P_{lac/ara}$ was cut from vector pZS*24 (Lutz and Bujard, 1997) at the AatII and EcoRI sites, and inserted between the AatII and MfeI sites of the promoter-less BAC vector. The 96 binding site array was inserted between the ClaI and MluI sites. The coding region for mRFP1 (including ribosome binding site and stop codon) was amplified from pRSET-B (Campbell et al., 2002) and inserted into the BAC2 ClaI site. The resulting vector is an F-based plasmid, with a $P_{lac/ara}$ promoter controlling the production of a message containing mRFP1 upstream of the 96 MS2 binding site array. To create a construct with the reverse order of coding region and binding sites array, mRFP1 was amplified and inserted into the MluI site.

Construction of the P_{RM} Reporter

The immunity region (position 35.4–38.4 kb [Hendrix, 1983]) of wild-type bacteriophage lambda (λ_{PAPA}, gift of R. Weisberg) was amplified with primers containing BamHI and MluI sites and inserted into the promoter-less BAC vector. The resulting plasmid, minus the *rexAB* region, was amplified with primers containing NheI and BstBI sites. A 48 binding site array previously cloned into a pBLUESCRIPT plasmid (Golding and Cox, 2004) was excised using ClaI and XbaI. The plasmid and insert were ligated and cloned to yield a BAC vector carrying λ_{imm}(*rexAB*::bs48).

Bacterial Growth and Induction

Cells were grown in LB (Miller, 1992), supplemented by antibiotics according to the specific plasmids markers. For induction of protein and RNA, cells were grown overnight from a single colony, diluted 1:1000 into fresh medium, and grown with aeration at 37 ºC. To induce the production of the MS2-GFP tag, 100 ng/ml aTc was added. After ~45 min, a sufficient amount of protein is present for RNA detection. Detection is not sensitive to the exact induction level (see text). RNA target production was induced by various levels of arabinose (0%–0.1%) and IPTG (0–1 mM). Unless stated otherwise, cells were preincubated with arabinose to obtain full activation of the *ara* system before derepression of the *lac* component. Message levels were then tracked starting a few minutes after induction and up to many hours afterwards. To maintain exponential growth, cells were diluted into fresh prewarmed medium whenever the optical density approached OD_{600} ~0.5.

Microscopy and Image Analysis

At each time point, a few μl of culture was placed between a coverslip and a thin slab of 0.8% agarose containing LB. Microscopy was performed with a Nikon Eclipse (TE-2000-U, Nikon, Tokyo, Japan) inverted microscope equipped with a 100× (1.3 NA) objective and epifuorescence system. Filter sets used were B-2E/C (FITC) for GFP detection, and Y-2E/C (Texas Red) for mRFP1 detection. Images were taken with a Roper Cascade 512B camera (Photometrics, Tuscon, AZ) after an additional 4× magnification. Images were acquired using MetaView software (Universal Imaging, Downingtown, PA). Image processing used to recognize cells and fluorescent foci and measure fluorescence intensity was performed using the Image Processing Toolbox of MATLAB (The Mathworks, Natick, MA). Fluorescent images obtained through each filter were read into MATLAB in TIFF format and processed as follows (the source code is available upon request): a morphological opening operation (erosion followed by dilation) was performed to estimate the background level. The background image was then subtracted from the original image and the contrast adjusted. A binary version of the image was created by using automatic thresholding. This binary image was used to recognize individual bacteria in the picture. Falsely recognized objects were discarded based on criteria of size, axial ratio, and solidity. To identify fluorescent foci, a similar procedure was repeated within each bacterial cell, again using additional morphological parameters to decrease the number of false recognitions. Once the objects (cells and foci) were determined, measurements of green fluorescent levels of the cells and foci were performed

on the original unprocessed TIFF image. For measurement of protein levels (red fluorescence), only the cell-recognition procedure was used.

To obtain the values of green foci intensity (I_G) and red cell intensity (I_R), I_R was obtained by integrating the total fluorescence (photon flux per second) of the cell (red channel) and subtracting the background level in the same image. I_G was obtained by integrating the total fluorescence of foci in the cell (green channel) and subtracting the background (green) level in the same cell. The number of tagged transcripts in the cell was estimated by dividing I_G by the intensity of the first peak in the I_G histogram (see e.g., Figure 1D). At very low induction levels, only a single peak is detected, which corresponds to the intensity of a single tagged message (Golding and Cox, 2004).

Induction under the Microscope

Cell growth and induction of MS2-GFP was as described above. For observation of RNA induction, a few μl of culture was placed between a coverslip and a 1 mm thick slab of 1% agarose containing LB that had been preincubated overnight with IPTG (1 mM) and aTc (100 ng/ml). A series of fluorescent images was taken at 30 s intervals for at least 2 hr.

Stochastic Model for Transcription

The following model was implemented in MATLAB. A population of 500 cells, with a random distribution of cell ages, all with zero mRNA molecules, was "induced" at time $t = 0$ into a state where each cell had constant probability per unit time (k_1) of making a "burst" of transcripts. Each burst was exponentially distributed, with an average value b. Simulated data were collected from $t = 0$ to $t = 150$ min. During this time, cells divided, with generation time $\tau_g = 50$ min. At each cell division, the existing mRNA molecules were split between the daughter cells, with a binomial distribution for the copy number received by each cell. Protein production was modeled as a Poisson process, where each existing transcript can be translated into a protein with constant probability per unit time, and protein partition was modeled with binomial statistics. The rate of translation was chosen so as to reproduce the measured mRFP1 level in the cell.

Estimation of Transcript Numbers by QPCR

Cells were grown and induced as described above. Total RNA was isolated using an RNeasy kit (QIAGEN, Valencia, CA) according to the manufacturer's instructions. Primers for mRFP1 and for ribosomal 16S RNA were designed using Applied Biosystems Primer Express 2.0 software (Applied Biosystems, Foster City, CA) to yield amplicons of approximate length 100 bp. Reverse transcription was performed using the Superscript II Reverse Transcription kit (Invitrogen, Carlsbad, CA) and these primers. Regular PCR reactions were then performed to verify that proper cDNA products were created. Real-time PCR reactions were performed using SYBR Green Master Mix (Applied Biosystems) in an ABI Prism 6700 (Applied Biosystems). A standard curve was created by measuring the threshold-crossing cycle number (Ct) for a series of known dilutions of the different primers to verify that amplification efficiency was comparable. The standard curve for 16S rRNA was used to estimate the relative number of mRFP1 transcripts under different induction conditions. To translate these relative values into absolute copy numbers per cell, a value of 20,000 16S RNA molecules per cell was used (Neidhardt et al., 1990).

Supplemental Data

Supplemental Data include supplemental text and can be found with this article online at http://www.cell.com/cgi/content/full/123/6/1025/DC1/.

ACKNOWLEDGMENTS

We are grateful to T. Silhavy and M. Elowitz for critical reading of an early version of this manuscript. We thank R. Segev, R. Austin, J. Puchalla, and P. Wolanin for generous advice; D. Peabody, R. Tsien, P. Wolanin, and R. Weisberg for strains and plasmids; L. Guo for technical assistance; and all members of the Cox laboratory.

This work was supported by the STC Program of The National Science Foundation under Agreement No. ECS-9876771 and in part by National Institute of Health grant HG 001506. I.G. is a Lewis Thomas Fellow. J.P. was supported by a Royal Society Research Grant 2004/R1.

The authors dedicate this paper to Charles Yanofsky, who continues in his eightieth year to break new ground in gene regulation, and who inspired one of us to keep thinking about transcription.

Received: April 26, 2005
Revised: July 13, 2005
Accepted: September 22, 2005
Published: December 15, 2005

REFERENCES

Artsimovitch, I., and Landick, R. (2000). Pausing by bacterial RNA polymerase is mediated by mechanistically distinct classes of signals. Proc. Natl. Acad. Sci. USA *97*, 7090–7095.

Baker, R.F., and Yanofsky, C. (1968). The periodicity of RNA polymerase initiations: a new regulatory feature of transcription. Proc. Natl. Acad. Sci. USA *60*, 313–320.

Bar-Nahum, G., and Nudler, E. (2001). Isolation and characterization of sigma(70)-retaining transcription elongation complexes from *Escherichia coli*. Cell *106*, 443–451.

Beckwith, J.R., and Zipser, D. (1970). The Lactose Operon (Cold Spring Harbor, NY: Cold Spring Harbor Laboratory Press).

Benzer, S. (1953). Induced synthesis of enzymes in bacteria analyzed at the cellular level. Biochim. Biophys. Acta *11*, 383–395.

Berg, O.G. (1978). A model for the statistical fluctuations of protein numbers in a microbial population. J. Theor. Biol. *71*, 587–603.

Bernstein, J.A., Khodursky, A.B., Lin, P.H., Lin-Chao, S., and Cohen, S.N. (2002). Global analysis of mRNA decay and abundance in Escherichia coli at single-gene resolution using two-color fluorescent DNA microarrays. Proc. Natl. Acad. Sci. USA *99*, 9697–9702.

Blake, W.J., Kaern, M., Cantor, C.R., and Collins, J.J. (2003). Noise in eukaryotic gene expression. Nature *422*, 633–637.

Bremer, H., and Ehrenberg, M. (1995). Guanosine tetraphosphate as a global regulator of bacterial RNA synthesis: a model involving RNA polymerase pausing and queuing. Biochim. Biophys. Acta *1262*, 15–36.

Campbell, R.E., Tour, O., Palmer, A.E., Steinbach, P.A., Baird, G.S., Zacharias, D.A., and Tsien, R.Y. (2002). A monomeric red fluorescent protein. Proc. Natl. Acad. Sci. USA *99*, 7877–7882.

Contesse, G., Crepin, M., and Gros, F. (1969). Rhythmic transcription of the Escherichia coli lactose operon. Bull. Soc. Chim. Biol. (Paris) *51*, 1445–1452.

Delbruck, M. (1940). Statistical fluctuations in autocatalytic reactions. J. Chem. Phys. *8*, 120–124.

Dieci, G., and Sentenac, A. (2003). Detours and shortcuts to transcription reinitiation. Trends Biochem. Sci. *28*, 202–209.

Elowitz, M.B., Levine, A.J., Siggia, E.D., and Swain, P.S. (2002). Stochastic gene expression in a single cell. Science *297*, 1183–1186.

Epshtein, V., and Nudler, E. (2003). Cooperation between RNA polymerase molecules in transcription elongation. Science *300*, 801–805.

Foe, V.E. (1978). Modulation of ribosomal RNA synthesis in Oncopeltus fasciatus: an electron microscopic study of the relationship between changes in chromatin structure and transcriptional activity. Cold Spring Harb. Symp. Quant. Biol. *42*, 723–740.

Gardiner, C.W. (2004). Handbook of Stochastic Methods: For Physics, Chemistry, and the Natural Sciences, 3rd Edition (New York: Springer).

Gillespie, D.T. (1977). Exact stochastic simulation of coupled chemical-reactions. J. Phys. Chem. *81*, 2340–2361.

Golding, I., and Cox, E.C. (2004). RNA dynamics in live Escherichia coli cells. Proc. Natl. Acad. Sci. USA *101*, 11310–11315.

Gowrishankar, J., and Harinarayanan, R. (2004). Why is transcription coupled to translation in bacteria? Mol. Microbiol. *54*, 598–603.

Guptasarma, P. (1995). Does replication-induced transcription regulate synthesis of the myriad low copy number proteins of Escherichia coli. Bioessays *17*, 987–997.

Guptasarma, P. (1996). Cooperative relaxation of supercoils and periodic transcriptional initiation within polymerase batteries. Bioessays *18*, 325–332.

Hendrix, R.W. (1983). Lambda II (Cold Spring Harbor, NY: Cold Spring Harbor Laboratory Press).

Imamoto, F. (1968). On the initiation of transcription of the tryptophan operon in Escherichia coli. Proc. Natl. Acad. Sci. USA *60*, 305–312.

Johansson, H.E., Dertinger, D., LeCuyer, K.A., Behlen, L.S., Greef, C.H., and Uhlenbeck, O.C. (1998). A thermodynamic analysis of the sequence-specific binding of RNA by bacteriophage MS2 coat protein. Proc. Natl. Acad. Sci. USA *95*, 9244–9249.

Kaern, M., Elston, T.C., Blake, W.J., and Collins, J.J. (2005). Stochasticity in gene expression: from theories to phenotypes. Nat. Rev. Genet. *6*, 451–464.

Kennell, D., and Riezman, H. (1977). Transcription and translation initiation frequencies of the Escherichia coli lac operon. J. Mol. Biol. *114*, 1–21.

Kepler, T.B., and Elston, T.C. (2001). Stochasticity in transcriptional regulation: origins, consequences, and mathematical representations. Biophys. J. *81*, 3116–3136.

Khodursky, A.B., Peter, B.J., Cozzarelli, N.R., Botstein, D., Brown, P.O., and Yanofsky, C. (2000). DNA microarray analysis of gene expression in response to physiological and genetic changes that affect tryptophan metabolism in Escherichia coli. Proc. Natl. Acad. Sci. USA *97*, 12170–12175.

Le, T.T., Harlepp, S., Guet, C.C., Dittmar, K., Emonet, T., Pan, T., and Cluzel, P. (2005). Real-time RNA profiling within a single bacterium. Proc. Natl. Acad. Sci. USA *102*, 9160–9164.

Lee, P.S., Shaw, L.B., Choe, L.H., Mehra, A., Hatzimanikatis, V., and Lee, K.H. (2003). Insights into the relation between mRNA and protein expression patterns: II. experimental observations in Escherichia coli. Biotechnol. Bioeng. *84*, 834–841.

Li, Y., and Altman, S. (2004). Polarity effects in the lactose operon of Escherichia coli. J. Mol. Biol. *339*, 31–39.

Lutz, R., and Bujard, H. (1997). Independent and tight regulation of transcriptional units in Escherichia coli via the LacR/O, the TetR/O and AraC/I1–I2 regulatory elements. Nucleic Acids Res. *25*, 1203–1210.

Mathews, C.K., Van Holde, K.E., and Ahern, K.G. (2000). Biochemistry, 3rd Edition (San Francisco: Benjamin Cummings).

McAdams, H.H., and Arkin, A. (1997). Stochastic mechanisms in gene expression. Proc. Natl. Acad. Sci. USA *94*, 814–819.

Miller, J.H. (1992). A Short Course in Bacterial Genetics: A Laboratory Manual and Handbook for Escherichia coli and Related Bacteria (Plainview, NY: Cold Spring Harbor Laboratory Press).

Neidhardt, F.C. (1996). Escherichia coli and Salmonella: Cellular and Molecular Biology, 2nd Edition (Washington, DC: ASM Press).

Neidhardt, F.C., Ingraham, J.L., and Schaechter, M. (1990). Physiology of the Bacterial cell: A Molecular Approach (Sunderland, MA: Sinauer Associates).

Novick, A., and Weiner, M. (1957). Enzyme induction as an all-or-none phenomenon. Proc. Natl. Acad. Sci. USA *43*, 553–566.

Ozbudak, E.M., Thattai, M., Kurtser, I., Grossman, A.D., and van Oudenaarden, A. (2002). Regulation of noise in the expression of a single gene. Nat. Genet. *31*, 69–73.

Paulsson, J. (2004). Summing up the noise in gene networks. Nature *427*, 415–418.

Peccoud, J., and Ycart, B. (1995). Markovian modeling of gene-product synthesis. Theor. Popul. Biol. *48*, 222–234.

Raser, J.M., and O'Shea, E.K. (2004). Control of stochasticity in eukaryotic gene expression. Science *304*, 1811–1814.

Rigney, D.R. (1979a). Note on the kinetics and stochastics of induced protein synthesis as influenced by various models for messenger RNA degradation. J. Theor. Biol. *79*, 247–257.

Rigney, D.R. (1979b). Stochastic model of constitutive protein levels in growing and dividing bacterial cells. J. Theor. Biol. *76*, 453–480.

Rosenfeld, N., Young, J.W., Alon, U., Swain, P.S., and Elowitz, M.B. (2005). Gene regulation at the single-cell level. Science *307*, 1962–1965.

Ryals, J., Little, R., and Bremer, H. (1982). Temperature dependence of RNA synthesis parameters in Escherichia coli. J. Bacteriol. *151*, 879–887.

Sasai, M., and Wolynes, P.G. (2003). Stochastic gene expression as a many-body problem. Proc. Natl. Acad. Sci. USA *100*, 2374–2379.

Schrodinger, E. (1944). What Is Life? The Physical Aspect of the Living Cell (Cambridge: Cambridge University Press).

Shaevitz, J.W., Abbondanzieri, E.A., Landick, R., and Block, S.M. (2003). Backtracking by single RNA polymerase molecules observed at near-base-pair resolution. Nature *426*, 684–687.

Shundrovsky, A., Santangelo, T.J., Roberts, J.W., and Wang, M.D. (2004). A single-molecule technique to study sequence-dependent transcription pausing. Biophys. J. *87*, 3945–3953.

Siegele, D.A., and Hu, J.C. (1997). Gene expression from plasmids containing the araBAD promoter at subsaturating inducer concentrations represents mixed populations. Proc. Natl. Acad. Sci. USA *94*, 8168–8172.

Swain, P.S., Elowitz, M.B., and Siggia, E.D. (2002). Intrinsic and extrinsic contributions to stochasticity in gene expression. Proc. Natl. Acad. Sci. USA *99*, 12795–12800.

Tapaswi, P.K., Roychoudhury, R.K., and Prasad, T. (1987). A stochastic-model of gene activation and RNA-synthesis during embryogenesis. Sankhya—the Indian Journal of Statistics Series B *49*, 51–67.

Thattai, M., and van Oudenaarden, A. (2001). Intrinsic noise in gene regulatory networks. Proc. Natl. Acad. Sci. USA *98*, 8614–8619.

Tolker-Nielsen, T., Holmstrom, K., Boe, L., and Molin, S. (1998). Non-genetic population heterogeneity studied by in situ polymerase chain reaction. Mol. Microbiol. *27*, 1099–1105.

Uptain, S.M., Kane, C.M., and Chamberlin, M.J. (1997). Basic mechanisms of transcript elongation and its regulation. Annu. Rev. Biochem. *66*, 117–172.

van Kampen, N.G. (1992). Stochastic Processes in Physics and Chemistry, Rev. and Enlarged Edition (Amsterdam: North-Holland).

Yanofsky, C., and Ito, J. (1966). Nonsense codons and polarity in the tryptophan operon. J. Mol. Biol. *21*, 313–334.